

Performance Analysis of Fractured Wells with Stimulated Reservoir Volume in Coal Seam Reservoirs

Zhao Yu-long^{1*}, Zhang Lie-Hui¹, Feng Guo-Qing¹, Zhang Bo-Ning¹ and Kang Bo²

¹ State Key Laboratory of Oil and Gas Reservoir Geology and Exploitation, Southwest Petroleum University, Chengdu, Sichuan 610500, P.R. China

² Chengdu North Petroleum Exploration and Development Technology LTD, Chengdu, Sichuan 610500, P.R. China

e-mail: 373104686@qq.com

* Corresponding author

Abstract — *CoalBed Methane (CBM), as one kind of unconventional gas, is an important energy resource, attracting industry interest in research and development. Using the Langmuir adsorption isotherm, Fick's law in the matrix and Darcy flow in cleat fractures, and treating the Stimulated Reservoir Volume (SRV) induced by hydraulic fracturing as a radial composite model, the continuous linear source function with constant production is derived by the methods of the Laplace transform and Duhamel theory. Based on the linear source function, semi-analytical solutions are obtained for a fractured vertical well producing at a constant production rate or constant bottom-hole pressure. With the help of the Stehfest numerical algorithm and computer programming, the well test and rate decline type curves are obtained, and the key flow regimes of fractured CBM wells are: wellbore storage, linear flow in SRV region, diffusion flow and later pseudo-radial flow. Finally, we analyze the effect of various parameters, such as the Langmuir volume, radius and permeability in the SRV region, on the production performance. The research results concluded in this paper have significant importance in terms of the development, well test interpretations and production performance analysis of unconventional gas.*

Résumé — **Analyse des performances de puits fracturés avec un volume de réservoir stimulé dans des gisements de charbon** — Le gaz de houille (*CoalBed Methane*, CBM), en tant que gaz non conventionnel, est une ressource d'énergie importante, qui attire l'intérêt industriel en matière de recherche et de développement. En utilisant l'isotherme d'adsorption de Langmuir, la loi de Fick dans la matrice et le flux de Darcy dans les fractures clivées, et en traitant le volume de réservoir stimulé (*Stimulated Reservoir Volume*, SRV) induit par la fracture hydraulique comme un modèle composite radial, la fonction de source linéaire continue avec une production constante est obtenue par les méthodes de la transformée de Laplace et de la théorie de Duhamel. Sur la base de la fonction de source linéaire, des solutions semi-analytiques sont obtenues pour un puits vertical fracturé produisant à un taux de production constant ou à une pression de fond constante. En s'aidant de l'algorithme numérique de Stehfest et de la programmation informatique, des courbes de test de puits et de déclin de taux de production sont obtenues, et les régimes d'écoulement clés des puits CBM fracturés sont les suivants : stockage de puits de forage, flux linéaire dans la zone SRV, flux de diffusion et flux pseudo-radial ultérieur. Enfin, nous analysons l'effet de différents paramètres, tels que le

Greek Variables Equations

$\Delta\bar{\psi}_{1f}$	Pseudo-pressure of the inner fracture system in Laplace space
μ	Gas viscosity (cp)
μ_{gi}	Gas viscosity, evaluated in the initial pressure conditions (cp)
α	Conversion factor, and $\alpha = 3.684 \times 10^{-3}$ for practical units
\emptyset_{1f}	Porosity of the fracture system in the SRV region, fraction
\emptyset_{2f}	Porosity of the fracture system in the outer region, fraction
ρ_{sc}	Fluid density under the standard conditions (g/m^3)
$\psi(p)$	Real gas pseudo-pressure (MPa^2/cp)
ψ_{fi}	Pseudo-pressure in initial fracture conditions (MPa^2/cp)
ψ_{wf}	Pseudo-pressure of bottom-hole pressure (MPa^2/cp)
$\psi_L(p_i)$	Langmuir pseudo-pressure constant (MPa^2/cp)
ω_1	Storativity ratio of the inner region (-)
ω_2	Storativity ratio of the outer region (-)
λ	Dimensionless transfer constant, defined in Equation (17)
τ	Sorption time (h)
Λ	Parameters defined in Equation (22)
σ	Ad- and desorption coefficients, defined in Equation (23)
ε	Variable

Subscripts

a	Pseudo
D	Dimensionless variable
f	Fracture system
mD	Matrix dimensionless
wD	Wellbore dimensionless
sc	Standard conditions
1	Inner region
2	Outer region

Superscripts

–	Laplace transform
---	-------------------

Operator

$L^{-1}[\]$	Laplace inverse transform operator
--------------	------------------------------------

INTRODUCTION

Coal seams, together with tight gas sands, Devonian shales and gas hydrates, are classified as unconventional gas reservoirs. Coal seams, similar to shale reservoirs, are known to be a source rock for natural gas. The gas stored in coal seams is primarily composed of methane, which is usually called CoalBed Methane (CBM). The contribution of CBM to unconventional gas reservoirs has played an important role in gas production all over the world. In the US, for example, the maximum annual production of CBM was 55.67 billion cubic meters in 2008, accounting for 9.75% of its domestic gas production. Although the subsequent annual production from 2009 to 2011 was continuously declining, the production of CBM is still expected to grow dramatically in the future with the economic recovery in the US (Source: US Energy Information Administration, Washington, DC; http://www.eia.gov/dnav/ng/hist/rngr52nus_1a.htm).

Due to the large internal surface area of coal seams, a significant amount of gas is stored as adsorbed gas as well as free gas in the network of cleats, and the characteristics of the coal composition, reservoir temperature and pressure, and the development of cleats vary significantly from one coal bed to another. Therefore, each CBM reservoir has distinct transport behaviors and different producing methods. Well testing is a powerful technique to recognize the *in situ* characterization and evaluate the stimulation effect of oil and gas reservoirs, and has been widely implemented to determine the gas transport and sorption characteristics of coal beds (Bayles and Reznik, 1986). Therefore, a vital task for researchers is to establish various models to evaluate the properties of underground reservoirs.

The physical and mathematical models to describe gas transport in coal reservoirs are well known and have been studied in the past. King *et al.* (1986) described the mathematical and numerical developments for a series of finite difference models that simulate the simultaneous flow of water and gas through dual-porosity coal seams. Bumb and Mckee (1988) derived an approximate analytical solution for single-phase gas flow when gas exists both as free gas and adsorbed on the matrix. Ertekin and Sung (1989) established a single-phase mathematical model in radial-cylindrical coordinates to describe both unsteady-state sorption phenomena in the coal matrix and the coupled laminar gas transport in the fracture network. Anbarci and Ertekin (1990) derived a single-phase flow equation for coalbed methane that includes non-equilibrium sorption phenomena in the coal matrix and laminar gas transport in the cleat system with kinds of outer and inner

boundary conditions. Rushing *et al.* (1991) developed a model to analyze the transient pressure response from slug tests in wells completed in multiple, hydraulically fractured coal seams. Engler and Rajtar (1992) presented an analytical solution for horizontal wells producing at constant rate in anisotropic, semi-infinite reservoirs by the Laplace and Fourier integral transform methods. Anbarci and Ertekin (1992) presented a solution package to describe the pressure transient behavior of coal reservoirs in the presence of a hydraulically fractured well. Kamal and Six (1993) presented a new analysis method for pressure transient testing in coal degasification projects. Sarkar and Rajtar (1994) developed a new semi-analytical solution to account for wellbore storage and skin effects on the pressure response of a horizontal well.

Later, Claudia and Joseph (2004) analyzed the production data by analytical solutions, which include analytical solutions for coalbed wells that took into account gas desorption from coal using isotherm data, analytical solutions for conventional gas reservoirs and Arp's decline curve analysis. Meng and Luke (2007) presented a rigorous dual-porosity model for gas reservoir flow incorporating adsorption behavior and obtained an analytical solution for diffusion within a matrix block. Clarkson (2009) and Clarkson *et al.* (2013) reported the production data and pressure transient analysis for coalbed methane wells. Hu *et al.* (2009) developed a new mathematical model with the consideration of Klinkenberg effects on coalbed gas flow properties. Nie *et al.* (2012) established a mathematical model of a horizontal well in a coalbed reservoir with the consideration of pseudo-steady diffusion in the matrix and Darcy flow in the network of cleats to analyze the transient pressure and rate decline behaviors. Based on Fick's law in the matrix and Darcy flow in cleats and hydraulic fractures, Wang *et al.* (2013) presented a new semi-analytical model considering the effects of boundary conditions to investigate the transient pressure behavior for asymmetrically fractured wells in coal reservoirs.

In general, coal seam reservoirs have dual porosity, which is macro-pores in the natural fracture network and those in the coal matrix (Claudia and Joseph, 2004; Meng and Luke, 2007; Clarkson, 2009; Nie *et al.*, 2012; Clarkson *et al.*, 2013; Wang *et al.*, 2013). The production of CBM in coal beds can be cataloged into three stages:

- Darcy flow of CBM through the fracture network to the wellbore;
- desorption of the gas from the matrix-cleat surfaces;
- diffusion of CBM through the network of capillaries and micro-pores within the coal matrix to the

matrix-cleat interface (Anbarci and Ertekin, 1990, 1992).

Hydraulic fracturing is an effective well stimulation technique employed for production of oil and gas from damaged wells or from low-permeability reservoirs, and it has become a primary technique for CBM development (Rushing *et al.*, 1991; Anbarci and Ertekin, 1992; Wang *et al.*, 2013). With the development of drilling and fracturing equipment, Massive Hydraulic Fracturing (MHF) has been widely used in CBM wells, which activates and connects existing discrete or micro-seismic natural fractures. Due to the natural fracture network and unique rock mechanics properties of the coal beds, MHF of CBM wells always generates a fracture network around the well, which is usually called Stimulated Reservoir Volume (SRV). The SRV is always defined as the volume of a reservoir containing the fracture network and the main hydraulic fractures with which it is effectively stimulated for improved well performance.

Due to the well testing analysis is an effective method to understand the *in situ* characterization of coal beds and evaluate fracturing effectiveness, and most of the above literature on this subject models the CBM transport characteristics without taking into account the effect of the SRV on the fluid flow performance (Bayles and Reznik, 1986; King *et al.*, 1986; Bumb and McKee, 1988; Anbarci and Ertekin, 1990, 1992; Sarkar and Rajtar, 1994; Claudia and Joseph, 2004; Meng and Luke, 2007; Clarkson, 2009; Nie *et al.*, 2012; Clarkson *et al.*, 2013; Wang *et al.*, 2013). Therefore, we expect to establish the corresponding mathematical model for the fractured CBM well with the SRV captured. In this paper, we considered the Langmuir adsorption isotherm and pseudo-steady and transient diffusion in the matrix, and Darcy flow both in the outer natural fracture region and inner SRV region.

1 DESCRIPTION OF PHYSICAL AND MATHEMATICAL MODEL

1.1 Characteristics of CBM Reservoirs

The characteristics of CBM reservoirs differ from conventional gas reservoirs in several areas. Unlike conventional gas reservoirs, coal is both the reservoir rock and the source rock. Most of the gas adsorbs on the surface of the coal grains on which desorption will occur during the process of production. The coal seam was treated as a dual porosity system, with the cleats as macro-porosity of the system and the spherical matrix elements representing the micro-pore structure (Claudia and Joseph, 2004; Meng and Luke, 2007; Clarkson, 2009; Cai and Yu, 2011; Nie *et al.*, 2012;

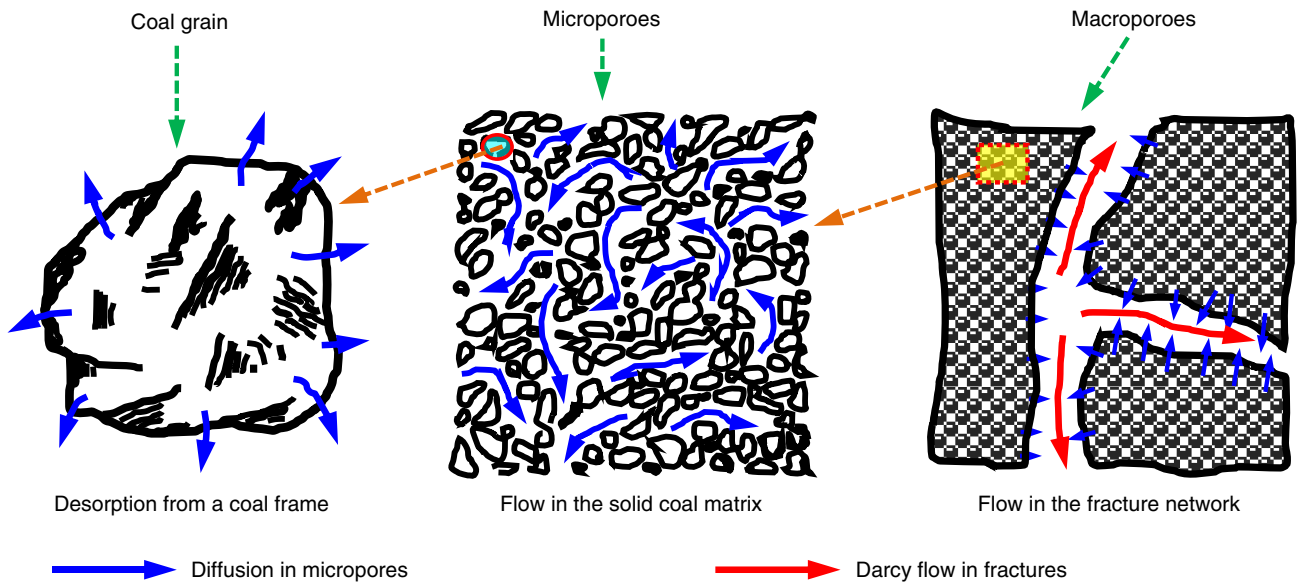


Figure 1
Schematic representation of methane flow through the coal seam.

Clarkson *et al.*, 2013; Wang *et al.*, 2013; Zhao *et al.*, 2012, 2013a, 2014). The seepage of the CBM through the porous media can be described as desorption and seepage flow (the schematic is shown in Fig. 1).

The equilibrium volumetric concentration which represents the amount of gas adsorbed in the matrix element is obtained using Langmuir’s isotherm (Langmuir, 1916; Zhao *et al.*, 2012, 2013a), which is:

$$V_E = V_L \frac{p}{p_L + p} \tag{1}$$

1.2 Continuous Linear Source Function

Although the natural fractures in a CBM reservoir are developed, the connectivity between the fractures is poor, which causes an ultra-low permeability for this reservoir as the effective permeability is a function of the conductivity, connectivity and density of fractures. Hydraulic fracturing is a common way to develop the low-permeability reservoir by injecting a mixture of liquid, sand and chemical into the formation at high pressure to create a high conductivity path around the well, which sometimes causes many induced small cracks around the main fractures (called induced fractures). As there is the development of natural fractures in a CBM reservoir, so we can use the dual-porosity model to describe it. Some of the natural fractures, including

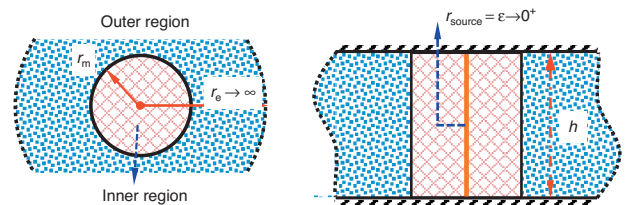


Figure 2
A schematic of a continuous line source in a radial composite reservoir.

connected and disconnected, may be connected by the induced hydraulic fractures, which causes a fracture network around the well called SRV. The induced fractures can effectively connect the natural fractures around the well, which significantly enhances the permeability of the fracture system. In order to describe a reservoir with developed natural fractures and the SRV around the well simply, we use a composite model and the inner region can be treated as the SRV caused by hydraulic fracturing (Fig. 2).

In order to make the problem more tractable, we made the following assumptions:

- a uniform thickness of h with a radius of the SRV region of r_m and a constant initial pressure p_i , and the upper and lower boundaries are sealed;

- the porosity, compressibility and permeability in the inner and outer regions are ϕ_{1f} , c_{f1} , k_{r1} ; ϕ_{2f} , c_{f2} , k_{r2} , respectively;
- the diffusion in the micro-pores obeys Fick's law (transient and pseudo-steady diffusion);
- the CBM flow in the macro-structure is only in the radial direction and obeys Darcy's law;
- the adsorbed gas is stored on the cleat surface and obeys the Langmuir isothermal adsorption equation;
- a fully fractured well with symmetrical wings located in the center of the inner region with the half length of x_f ;
- the well produces at a constant rate (q_{sc}) or a constant bottom-hole pressure (p_{wf}).

In order to obtain the pressure response expression of a fully penetrated fractured well in a CBM reservoir, we firstly derive the continuous line source function and then integrate the source function along the fractures (Zhao *et al.*, 2012, 2013a,b). The transport equation that describes single-phase, unsteady-state flow in the cleat fracture system can be obtained by performing a mass balance on a radial element volume (Ertekin and Sung, 1989; Anbarci and Ertekin, 1990, 1992; Sarkar and Rajtar, 1994).

For the Inner Region:

$$\frac{1}{r} \frac{\partial}{\partial r} \left(r \frac{k_{1f} p_{1f} M}{\mu Z_g RT} \frac{\partial p_{1f}}{\partial r} \right) = \frac{\phi_{1f} c_{1f} p_{1f} M}{3.6 Z_g RT} \frac{\partial p_{1f}}{\partial t} + q_1^* \quad (2)$$

q_1^* is the gas diffusion rate from the coal particles to the matrix micro-pore. As the matrix porosity is very small and few structural fractures developed, we can ignore the effect of compressibility of the matrix and fracture systems on the diffusion rate. Providing the diffusion follows the first law of diffusion, it yields:

$$q_1^* = \frac{\rho_{sc}}{3.6} \frac{\partial[(1 - \phi_{1f})V]}{\partial t} = \frac{Mp_{sc}(1 - \phi_{1f})}{3.6RT_{sc}} \frac{\partial V}{\partial t} \quad (3)$$

For the Outer Region:

$$\frac{1}{r} \frac{\partial}{\partial r} \left(r \frac{k_{2f} p_{2f} M}{\mu Z_g RT} \frac{\partial p_{2f}}{\partial r} \right) = \frac{\phi_{2f} c_{2f} p_{2f} M}{3.6 Z_g RT} \frac{\partial p_{2f}}{\partial t} + q_2^* \quad (4)$$

$$q_2^* = \frac{\rho_{sc}}{3.6} \frac{\partial[(1 - \phi_{2f})V]}{\partial t} = \frac{Mp_{sc}(1 - \phi_{2f})}{3.6RT_{sc}} \frac{\partial V}{\partial t} \quad (5)$$

$$\frac{\partial V}{\partial t} = \begin{cases} \frac{3D}{R_m} \frac{\partial V}{\partial r_m} \Big|_{r_m=R_m} & \text{for transient diffusion} \\ \frac{6D\pi^2}{R_m^2} (V_E - V) & \text{for pseudo-steady diffusion} \end{cases} \quad (6)$$

For a well with an infinite or closed outer boundary, we have:

$$p_{2f}(r, t) \Big|_{r \rightarrow \infty} = 0 \quad \text{for infinite} \quad (7)$$

$$\frac{\partial p_{2f}}{\partial r} \Big|_{r=r_c} = 0 \quad \text{for closed} \quad (8)$$

According to characteristics of the Dirac delta function (Zhao *et al.*, 2012), when the line source withdraws the fluid with an instantaneous rate (\hat{q}), the inner boundary condition becomes:

$$\lim_{\varepsilon \rightarrow 0^+} \frac{k_{1f}}{\mu} h \left(r \frac{\partial p_{1f}}{\partial r} \right)_{r=\varepsilon} = -\alpha \hat{q} \frac{Z p_{sc} T}{p_{1f} T_{sc}} \frac{k_{2f}}{\Lambda L^2} \quad (9)$$

The interface conditions defining pressure and flow rate continuity in the reservoir are expressed as follows:

$$p_{1f}(r, t) \Big|_{r=r_m} = p_{2f}(r, t) \Big|_{r=r_m} \quad (10)$$

and

$$p_{1f} \frac{\partial p_{1f}}{\partial r} \Big|_{r=r_m} = \frac{p_{2f}}{M_{12}} \frac{\partial p_{2f}}{\partial r} \Big|_{r=r_m} \quad (11)$$

Dimensionless Parameters

A pseudo-time function to account for the time dependence of gas viscosity and total system compressibility is defined as follows (Agarwal, 1979; Escobar *et al.*, 2013):

$$t_a = \int_{t_0}^t \frac{1}{\mu(t)c_g(t)} dt \quad (12)$$

For compressible fluids, the pseudo-pressure, $\psi(p)$, introduced by Agarwal (1979), is given by:

$$\psi(p) = 2 \int_0^p \frac{p}{\mu(p)Z(p)} dp \quad (13)$$

Dimensionless time is defined as:

$$t_D = \frac{3.6k_{2f}t_a}{\Lambda L^2}$$

The dimensionless storage of the inner and outer regions are:

$$\omega_1 = \frac{(\phi_1 \mu_{gi} c_{1l})_f}{\Lambda} \quad (15)$$

$$\omega_2 = \frac{(\phi_2 \mu_{gi} c_{2l})_f}{\Lambda} \quad (16)$$

The dimensionless transfer constant is defined as:

$$\lambda = \begin{cases} \frac{k_{2f}\tau}{\Lambda L^2} & \text{for transient diffusion} \\ \frac{k_{2f}\tau}{6\Lambda L^2} & \text{for pseudo-steady diffusion} \end{cases} \quad (17)$$

The desorption time constant is defined as:

$$\tau = \begin{cases} \frac{R_m^2}{D} & \text{for transient diffusion} \\ \frac{R_m^2}{\pi^2 D} & \text{for pseudo-steady diffusion} \end{cases} \quad (18)$$

And the other dimensionless parameters and groups are defined as follows:

$$M_{12} = \frac{k_{1f}/\mu_{gi}}{k_{2f}/\mu_{gi}} \quad (19)$$

$$r_{Dm} = \frac{r_m}{R_m} \quad (20)$$

$$r_D = \frac{r}{L} = \sqrt{(x_D - x_{wD})^2 + (y_D - y_{wD})^2} \quad (21)$$

$$\Lambda = \begin{cases} (\phi_f \mu_{gi} c_{tf})_{1+2} + \frac{6k_{f2}h}{\alpha q_{sc}} & \text{for transient diffusion} \\ (\phi_f \mu_{gi} c_{tf})_{1+2} + \frac{2k_{f2}h}{\alpha q_{sc}} & \text{for pseudo-steady diffusion} \end{cases} \quad (22)$$

Define the ad- and desorption coefficients σ as:

$$\sigma = \frac{V_L \psi_L(p_f)}{[\psi_L(p_f) + \psi(p_f)][\psi_L(p_f) + \psi(p_i)]} \frac{\alpha q_{sc} p_{sc} T}{k_{f2} h T_{sc}} \quad (23)$$

According to previous research results (King *et al.*, 1986; Anbarci and Ertekin, 1990, 1992; Sarkar and Rajtar, 1994; Claudia and Joseph, 2004; Clarkson, 2009; Clarkson *et al.*, 2013), the implicit expression of Λ can be treated as a constant at the initial pressure $[\psi(p_f) = \psi(p_i)]$.

Using the above dimensionless groups and combining Equations (2)-(6) with the corresponding boundary conditions when the well produces at a constant rate, detailed derivation of the instantaneous line source solution is shown in Appendix, which is:

$$\Delta \bar{\psi}_{1f} = \frac{p_{sc} T}{T_{sc}} \frac{3.6 k_{2f}}{\Lambda L^2} \frac{\alpha \hat{q}}{k_{1f} h} [K_0(\gamma_1 r_D) + A_C I_0(\gamma_1 r_D)] \quad (24)$$

where:

$$A_C = \frac{M_{12} \gamma_1 K_1(\gamma_1 r_{mD}) K_0(\gamma_2 r_{mD}) - \gamma_2 K_0(\gamma_1 r_{mD}) K_1(\gamma_2 r_{mD})}{M_{12} \gamma_1 I_1(\gamma_1 r_{mD}) K_0(\gamma_2 r_{mD}) + \gamma_2 I_0(\gamma_1 r_{mD}) K_1(\gamma_2 r_{mD})}$$

Using the Duhamel theory (Everdingen and Hurst, 1949), the continuous line source function can be obtained easily by:

$$\Delta \psi_{1f} = \frac{p_{sc} T}{T_{sc}} \frac{3.6 k_{2f}}{\Lambda L^2} \frac{\alpha}{k_{1f} h} \int_0^{t_D} q_{scL}(\tau) S_c(t_D - \tau) d\tau \quad (25)$$

where:

$$S_c = L^{-1} [\bar{S}_c]$$

$$\bar{S}_c = [K_0(\gamma_1 r_D) + A_C I_0(\gamma_1 r_D)]$$

Taking the Laplace transform with t_D in Equation (25), the continuous linear source function in composite dual-porosity CBM reservoir is:

$$\Delta \bar{\psi}_{1f} = \alpha \frac{p_{sc} T}{T_{sc}} \frac{\tilde{q}_{scL}}{k_{1f} h} [K_0(\gamma_1 r_D) + A_C I_0(\gamma_1 r_D)] \quad (26)$$

Hereto, the continuous linear source function in a radial composite CBM reservoir is obtained and some missing parameter groups are defined in Appendix.

2 SOLUTIONS OF A FRACTURED WELL IN A CBM RESERVOIR

2.1 Well Producing at a Constant Production Rate

In this section, the pressure transient behavior of a fractured vertical well with the SRV around the well is studied. The dual-porosity property of the coal beds is assumed and the unsteady-state desorption/diffusion formulation is used. The radial composite model consists of inner and zones with different properties. The fracture density of the inner zone is much better than the outer ones, which represents the SRV induced by the hydraulic fracturing. Figure 3 is the schematic of a fully penetrated fractured well in a CBM reservoir with the SRV around the well: to make the problem more tractable, the following assumptions are made:

- the reservoir is horizontal, with a uniform thickness of h , and the upper and lower boundaries are closed;
- a vertical fractured well is located at the center of the reservoir and the half fracture length is x_f ;

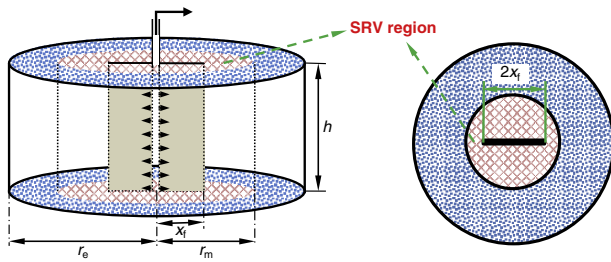


Figure 3

A schematic representation of a composite system with a vertically fractured well.

- the SRV region induced by hydraulic fracturing is a circular area with radius r_m ;
- the well produces at a constant rate q_{sc} , and the conductivity of the fracture is infinite.

According to the results of Gringarten *et al.* (1974), the transient pressure response solutions of wells with infinite conductive fractures can be obtained in the uniform flux fracture case by measuring the pressure drop at $x_D = 0.732$ in the fracture. The solution for a vertical uniform flux fractured well can be easily obtained by integrating the continuous linear source function obtained before to x_{wD} over the interval from -1 to 1 (Zeng and Zhao, 2010).

Define the dimensionless pressure as follows:

$$\bar{\psi}_{1fD} = \frac{k_{2f} h T_{sc}}{\alpha q_{sc} p_{sc} T} \Delta \bar{\psi}_{1f} \quad (27)$$

According to the relationship between the linear source strength (q_{scL}) and the well production rate (q_{sc}), which is $q_{sc} = 2 q_{scL} x_f$. Combine it with Equation (26) and Equation (27), and integrate the x_{wD} from -1 to 1 , yielding:

$$\bar{\psi}_{1fD} = \int_{-1}^1 \frac{1}{M_{12s}} [K_0(\gamma_1 r_D) + A_C I_0(\gamma_1 r_D)] dx_{wD} \quad (28)$$

The solution of Equation (28) does not consider near-wellbore damage from the hydraulic fracturing fluid or drilling; when considering the effect of the skin factor (S_{kin}), Equation (28) becomes:

$$\bar{\psi}_{SD} = \int_{-1}^1 \frac{1}{M_{12s}} [K_0(\gamma_1 r_D) + A_C I_0(\gamma_1 r_D)] dx_{wD} + \frac{S_{kin}}{s} \quad (29)$$

When the well produces at a constant rate, wellbore storage has a significant effect on the bottom-hole

pressure. According to the Duhamel principle (Everdingen and Hurst, 1949), the solution in Laplace space for modeling a fractured well in a CBM reservoir with the SRV can be obtained by:

$$\bar{\psi}_{wD} = \frac{\bar{\psi}_{SD}}{1 + C_D s^2 \bar{\psi}_{SD}} \quad (30)$$

2.2 Well Producing at a Constant Bottom-Hole Pressure

The above derivations and solutions are all based on the assumption that the well produces at a constant rate. However, for a CBM well producing at constant bottom hole pressure, the dimensionless production rate can also be derived with the similar method described above. Redefine the following dimensionless groups to replace the corresponding ones used above:

$$\Lambda = \begin{cases} (\phi_f \mu_{gi} c_{if})_{1+2} + \frac{6 p_{sc} T}{T_{sc} (\psi_i - \psi_{wf})} & \text{for transient diffusion} \\ (\phi_f \mu_{gi} c_{if})_{1+2} + \frac{2 p_{sc} T}{T_{sc} (\psi_i - \psi_{wf})} & \text{for pseudo-steady diffusion} \end{cases} \quad (31)$$

$$\sigma = \frac{V_L \psi_L(p_f)}{[\psi_L(p_f) + \psi(p_f)][\psi_L(p_f) + \psi(p_i)]} (\psi_i - \psi_{wf}) \quad (32)$$

According to previous research results (Everdingen and Hurst, 1949; Ozkan and Raghavan, 1991a, b), the solution of a CBM well producing at constant bottom-hole pressure is:

$$\bar{q}_D = \frac{1}{s^2 \bar{\psi}_{wD}} \quad (33)$$

where:

$$q_D = \frac{\alpha q_{sc} p_{sc} T}{k_{2f} h T_{sc} (\psi_{fi} - \psi_{wf})} \quad (34)$$

The standard log-log type curves for rate decline analysis (Blasingame *et al.*, 1991; Blasingame and Lee, 1994) can be obtained by defining the following expressions:

Dimensionless decline time:

$$t_{Dd} = \frac{t_D}{0.5(r_{eD}^2 - 1)[\ln(r_{eD}) - 0.5]} \quad (35)$$

Dimensionless decline rate function:

$$q_{Dd} = q_D [\ln(r_{eD}) - 0.5] \quad (36)$$

TABLE 1
Synthetic data used for the discussion of the results

Initial reservoir pressure, p_i (MPa)	15	Reservoir temperature, T (K)	320
Formation thickness, h (m)	60	Half fracture length, x_f (m)	50
Gas specific gravity, γ_g , fraction	0.65	Well production rate, q_{sc} (m ³ /d)	3×10^4
The radius of inner region, r_m	100	Equivalent radial of control area, r_c (m)	2500
Bottomhole pressure, p_{wf} (MPa)	4	Wellbore storage coefficient, C_D	10^{-5}
Skin factor, skin	0.1	The sorption time constant, τ (h)	2×10^5
Langmuir pressure, P_L (MPa)	1.5	Langmuir Volume, V_L (m ³ /m ³)	40
Inner region		Outer region	
Permeability, k_{if} (mD)	0.1	Permeability, k_{2f} (mD)	0.02
Porosity, ϕ_{1f}	0.02	Porosity, ϕ_{2f}	0.01
Total compressibility, C_{if1} (MPa ⁻¹)	1.0E-02	Total compressibility, C_{if2} (MPa ⁻¹)	1.0E-02

Dimensionless decline rate integral:

$$q_{Ddi} = \frac{\int_0^{t_{Dd}} q_{Dd}(\tau) d\tau}{t_{Dd}} \quad (37)$$

Dimensionless decline rate integral derivative:

$$q'_{Ddi} = -\frac{dq_{Ddi}}{d\ln(t_{Dd})} \quad (38)$$

3 WELL PERFORMANCE ANALYSIS

The dimensionless bottom-hole pseudo-pressure (ψ_{wD}) and the derivative ($d\psi_{wD}/dt_D$) can be obtained using the Stehfest numerical algorithm (Stehfest, 1970) to convert the $\bar{\psi}_{wD}$ back into ψ_{wD} . So, we can obtain the standard log-log type curves of well test analysis of ψ_{wD} and $\psi'_{wD} \times t_D/C_D$ versus t_D/C_D .

The standard rate decline curves of q_D versus t_D can also be obtained in the same way as the well testing type curves described above, and then by transforming them into real space through Equations (14) and (34) we can obtain the well production performance in real space. By substituting q_D and t_D into Equations (35-38) the standard log-log transient rate decline curves of q_{Ddi} and q'_{Ddi} versus t_{Dd} can be obtained (Blasingame *et al.*, 1991; Blasingame and Lee, 1994).

3.1 Type Curves for CBM Fractured Wells

Well testing as well as transient rate decline curves are very interesting to petroleum engineers, as they can

reflect the characteristics of the reservoirs and fluid flow behavior, and evaluate the effect of well stimulation. Also, using the type curve matching technology, the engineers can recognize the flow characteristics for a real reservoir and obtain the related property parameters, such as permeability, skin factor, control radial, fracture length, etc.

In this paper, we use the synthetic data in Table 1 to analyze the pressure response and the rate decline of the mathematical model derived in this paper; the results are shown in Figures 4-12.

Figures 4, 7, 9 and 11 show pseudo-pressure and pseudo-pressure derivative type curves of a fractured CBM well with the induced SRV. It can be found that the curves can be classified into the following flow periods.

Stage 1 Early wellbore storage, which is characterized by a unit slope line in both the pseudo-pressure and pseudo-pressure derivative curves (Stage 1 in Fig. 4).

Stage 2 A transition flow period between wellbore storage and the linear flow period in the SRV (Stage 2 in Fig. 4); the derivative curves in this stage are like a hump.

Stage 3 Linear flow in the SRV region, which is characterized by a half slope in both pseudo-pressure and pseudo-pressure derivative curves on a log-log scale. As the duration of this flow period is short, sometimes it will be masked by the wellbore storage effect of large C_D . Comparing this flow period of pseudo-steady diffusion

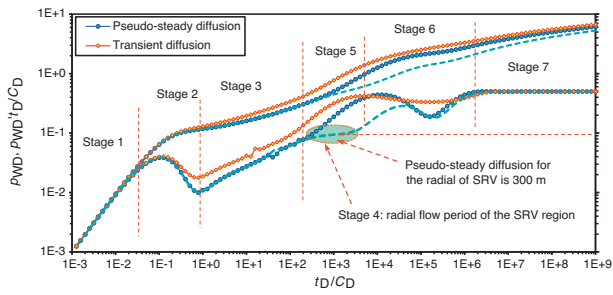


Figure 4
Comparison of the pseudo-steady and transient diffusion models on well test type curves.

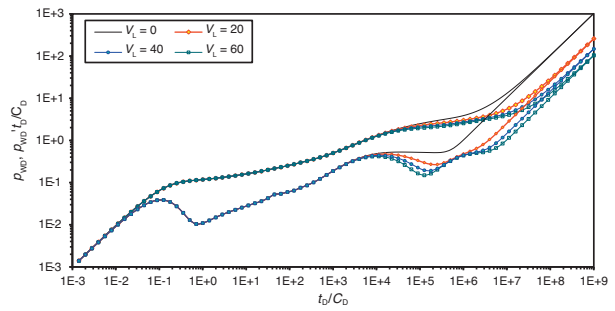


Figure 7
Effect of Langmuir Volume (V_L) on well testing type curves.

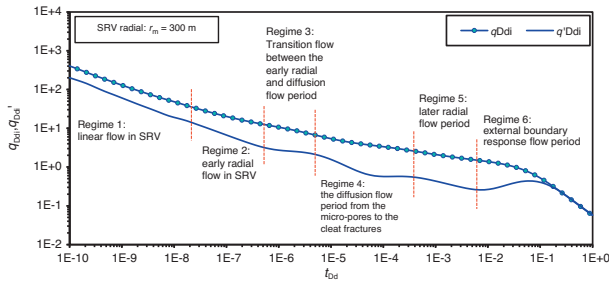


Figure 5
Transient rate decline type curves of a CBM fractured well with the SRV with pseudo-steady diffusion.

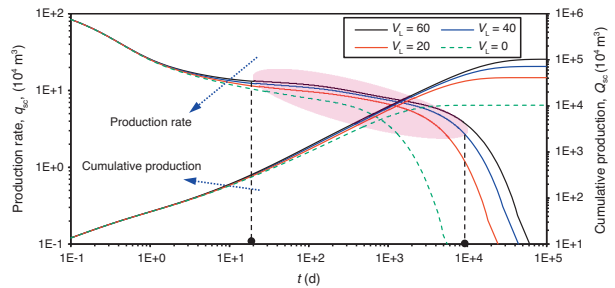


Figure 8
Effect of Langmuir Volume (V_L) on well production performance.

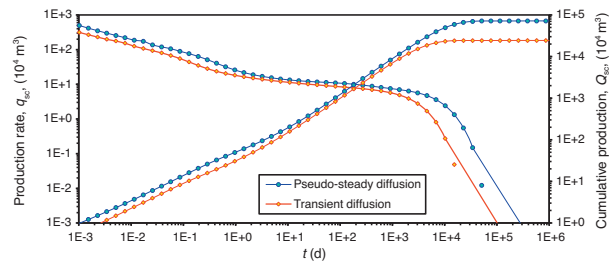


Figure 6
Comparison of the pseudo-steady and transient diffusion models on well production performance.

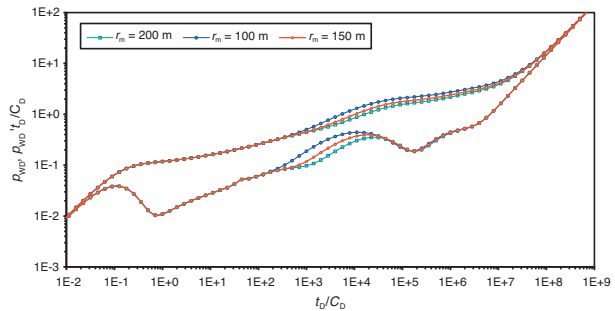


Figure 9
Effect of the SRV radial (r_m) on well testing type curves.

with the transient diffusion (Stage 3 in Fig. 4), it can be seen that the transient diffusion needs a higher pressure drop than the pseudo-steady diffusion curves when the well produces at a constant production rate. The gas adsorbed on the matrix particle surface can desorb and diffuse to the cleat fractures instantaneously for the pseudo-steady diffusion model. However, for

the transient diffusion model, the gas diffusion needs some time to complete, so the pressure drop is relatively small for steady-state diffusion compared with the transient diffusion model. The above reason can also explain why the production rate and cumulative production for transient diffusion are lower than the pseudo-steady model, as shown in Figure 6.

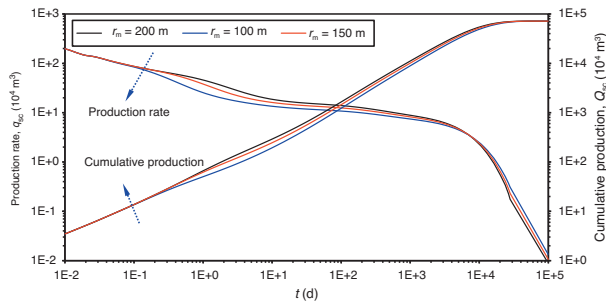


Figure 10
Effect of the SRV radial (r_m) on well production performance.

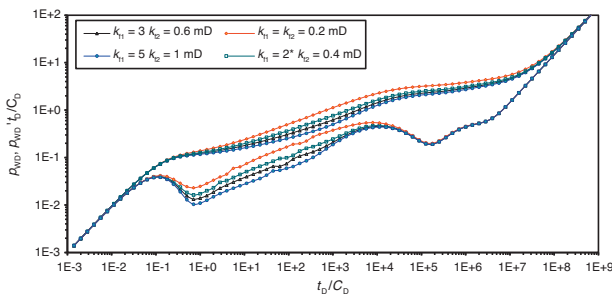


Figure 11
Effect of permeability in the SRV (k_{f1}) on well testing type curves.

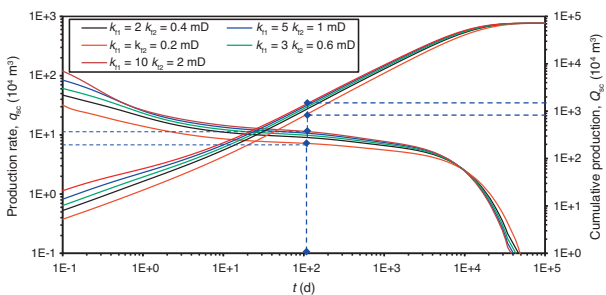


Figure 12
Effect of permeability in the SRV (k_{f1}) on well production performance.

Stage 4 Radial flow period in the SRV region; this flow period theoretically exists when the ratio of the SRV radial to the half fracture length is not big enough. As the half fracture length used in this paper is 50 m and the SRV radial is 100 m, the duration of this flow period is too short to be observed. In order to prove the existence of this

flow period and analyze its characteristics, we plot another type curve with the assumption that the SRV radial is 300 m (this situation is shown with the dashed line in Fig. 4), which is characterized by a horizontal line with the value of $1/(2 \times M_{12})$ (Stage 4 in Fig. 4).

Stage 5 The diffusion flow period from the micro-pores to the cleat fractures (Stage 5 in Fig. 4). In this flow period, the diffusion/desorption rate becomes more significant compared with the fluid supply in the cleat fractures; the production is mainly dominated by the depletion of micro-pores in the matrix. When the diffusion model is pseudo-steady, the derivative curves have a V-sharp below the straight line. It is the same for the interporosity flow period in natural fractured reservoirs. However for the transient diffusion model, the trough is much gentler.

Stage 6 The later pseudo radial flow period, for which the derivative curves are characterized by a horizontal line (its value is 0.5, Stage 6 in Fig. 4). During this flow period, the fluid transfer between micro-pores and cleat fractures has gone up to a state of dynamic balance. If the outer boundary is not infinite but closed, the derivative curves will gradually be upward with the slope of unit (this flow period can be obtained in Fig. 7, 9 and 11).

Figure 5 shows a fractured CBM well with pseudo-steady diffusion producing at a constant bottom-hole pressure in a coalbed reservoir with a closed outer boundary. The transient rate decline type curves can also be divided into the following six flow periods shown in Figure 5.

3.2 Parameters Affecting Well Pressure and Production Performance

Various parameters have a significant influence on the shape of well testing type curves and on the well production performance, which is also the main objective of production engineers. Only by understanding the effect of these parameters on well performance can more accurate results be obtained from well test analysis.

Figures 7 and 8 show the effect of Langmuir volume (V_L) on well testing type curves and production performance with a closed outer boundary condition. The Langmuir volume is defined as the maximum amount of gas that adsorbed on the matrix particle at infinite pressure. So, the bigger the V_L , the more gas will diffuse from the micro-pores to the cleat fractures with a constant pressure drop.

With all other parameters being constant, V_L has a primary effect on the starting time of the transition flow and external boundaries-dominated flow period, and the depth of the trough (Fig. 7). The bigger the V_L , the earlier the transition, the later the pseudo-radial flow arrives, and the deeper the trough. For $V_L = 0$, the characteristics of derivative pressure curves become the same as the traditional homogeneous gas reservoir with a fractured well. As V_L represents the gas desorption capacity of the CBM reservoir, when the well produces at a constant bottom-hole pressure, the more gas will desorb and diffuse to the fractures, the bigger the V_L and the greater the production will be (Fig. 9). From the marked elliptical area in Figure 8, we can see that when $V_L = 40 \text{ m}^3/\text{m}^3$, the duration of the plateau production is nearly 30 years, the average production rate is about $7.5 \times 10^4 \text{ m}^3/\text{d}$, and the cumulative production at the end of this time period is up to 630 million m^3 . However, for $V_L = 0 \text{ m}^3/\text{m}^3$, which means no adsorbed gas stored on the matrix particle (as shown by the dashed line in Fig. 8), the production rate of the well declines quickly after 2-3 years. This phenomenon can explain why the CBM well and shale gas well have a long stable production period compared with the conventional reservoir.

Figures 9 and 10 show the effect of the SRV radial (r_m) on the well pressure and the production performance. The new concept of the “Fracture network” fracturing technique was put forward for the ultra-low permeability reservoir and the unconventional gas reservoir, such as CBM and shale, which is also called the SRV region. A large value of the SRV area is always expected by engineers and can lead to considerable economic profit. For the well testing type curves, r_m mainly affects the duration of the radial flow period of the SRV region. The larger the r_m , the longer the duration will be (Fig. 9). When a well produces at constant bottom-hole pressure, r_m has a significant effect on the well production rate. The production rate and cumulative production will coincide at the beginning but differ after the pressure wave propagation to the interface. A larger r_m will form a large seepage surface from the formation to the SRV region, which will result in a higher production rate. However, when a well produces at the end of its life, the same cumulative production will be obtained (according to the material balance theory, when other parameters are kept constant, no matter how the value of r_m changes, the control reserve of the well is the same) (Fig. 10).

Figures 11 and 12 present the pressure and production performance with different permeability of the SRV (k_{f1}). A large k_{f1} presents a development of the fracture network. When a well produces at a constant rate, the larger the k_{f1} , the smaller the production drop will be and the lower the location of the derivative curves will

be on the log-log type curve (Fig. 11). For wells producing with a constant bottom-hole pressure, the bigger the k_{f1} , the higher the production rate. For example, after 100 days of production, the production rate will be nearly $10.2 \times 10^4 \text{ m}^3/\text{d}$ and the cumulative production is nearly $8 \times 10^6 \text{ m}^3$ for $k_{f1} = 10k_{f2} = 2 \text{ mD}$, but for a well without the SRV ($k_{f1} = k_{f2} = 0.2 \text{ mD}$), the rate is only $7 \times 10^4 \text{ m}^3/\text{d}$ and cumulative production is $10.8 \times 10^6 \text{ m}^3$. According to the data described above, the incremental production rate and cumulative production are both considerable.

CONCLUSIONS

In this paper, we investigated a comprehensive transport model for fractured CBM wells. With the assumption that a radial composite model with the inner region representing the SRV region induced by hydraulic fracturing is used, the solutions of this model at a constant production rate or bottom-hole pressure are obtained. Through the above analysis, the following conclusions can be summarized:

1. A mathematical model with multiple migration mechanisms to describe the fluid flow in the CBM reservoir is established, and the solutions of a fractured well with the SRV induced by hydraulic fracturing are obtained;
2. Well testing type curves and rate decline curves can be used to recognize the gas transport characteristics of CBM with different flow regimes. Compared with the conventional model, there is a trough on the pseudo-pressure derivative curves to reflect desorption and diffusion of CBM from the micro-pores to the cleat fractures;
3. The production rate and cumulative production for fractured wells with the SRV is much higher than the traditional single fracture well. And the larger the SRV radial and permeability, the higher the production rate will be;
4. Different parameters that govern the transport represent different physical characteristics, and also have different effects on the type of curves. As Langmuir Volume (V_L) represents the adsorption capacity of CBM, the bigger the V_L , and the deeper the trough will be;
5. The models and the results obtained in this paper give significant information on well tests and on the rate decline analysis of CBM wells.

ACKNOWLEDGMENTS

This work was supported by the National Science Fund for Distinguished Young Scholars of China (Grant

No. 51125019) and the Natural Science Foundation of China (Grant No. 51374181). The authors would also like to thank the reviewers and editors whose critical comments were very helpful in preparing this article.

REFERENCES

- Agarwal G. (1979) Real Gas Pseudo-time a New Function for Pressure Buildup Analysis of MHF Gas Wells, *54th Technical Conference and Exhibition of the Society of Petroleum Engineers of AIME*, Las Vegas, NV, 23-26 Sept., *SPE Paper* 8279-MS.
- Anbarci K., Ertekin T. (1990) A Comprehensive Study of Pressure Transient Analysis with Sorption Phenomena for Single-phase Gas Flow in Coal Seams, *65th annual Technical Conference and Exhibition of the Society of Petroleum Engineers*, New Orleans, LA, 23-26 Sept., *SPE Paper* 20568.
- Anbarci K., Ertekin K. (1992) Pressure Transient Behavior of Fractured Wells in Coalbed Reservoirs, *SPE Annual Technical Conference and Exhibition*, Washington, DC, 4-7 Oct., *SPE Paper* 24703-MS.
- Bayles G.A., Reznik A.A. (1986) Pressure Transient Analysis of Methane Production from Coal Beds: An Analytical Approach, *SPE Unconventional Gas Technology Symposium*, Louisville, Kentucky, 18-21 May, *SPE Paper* 15226-MS.
- Blasingame T.A., McCray T.L., Lee W.J. (1991) Decline Curve Analysis for Variable Pressure Drop/Variable Flow Rate Systems, *SPE Gas Technology Symposium*, Houston, Texas, 22-24 Jan., *SPE Paper* 21513-MS.
- Blasingame T.A., Lee W.J. (1994) The Variable-rate Reservoir Limits Testing of Gas Wells, *SPE Gas Technology Symposium*, Dallas, Texas, 13-15 June, *SPE Paper* 17708-MS.
- Bumb A.C., Mckee C.R. (1988) Gas-well Testing in the Presence of Desorption for Coalbed Methane and Devonian Shale, *SPE Formation Evaluation* 3, 1, 179-185.
- Cai J.C., Yu B.M. (2011) A Discussion of the Effect of Tortuosity on the Capillary Imbibition in Porous Media, *Transp. Porous Media* 89, 2, 251-263.
- Clarkson C.R. (2009) Case Study: Production Data and Pressure Transient Analysis of Horseshoe Canyon CBM wells, *Journal of Canadian Petroleum Technology* 48, 10, 27-38.
- Clarkson C.R., Behmanesh H., Chorney L. (2013) Production-data and Pressure-transient Analysis of Horseshoe Canyon Coalbed-methane Wells, Part : Accounting for Dynamic Skin, *Journal of Canadian Petroleum Technology* 52, 1, 41-53.
- Claudia L.P., Joseph P. (2004) Production Analysis of Coalbed Wells Using Analytical Transient Solutions, *SPE Eastern Regional Meeting*, Charleston, West Virginia, 15-17 Sept., *SPE Paper* 91447-MS.
- Engler T.W., Rajtar, J.M. (1992) Pressure Transient Testing of Horizontal Wells in Coalbed Reservoirs, *SPE Rocky Mountain Regional Meeting*, Casper, Wyoming, 18-21 May, *SPE Paper* 24374-MS.
- Ertekin T., Sung W. (1989) Pressure Transient Analysis of Coal Seams in the Presence of Multi-mechanistic Flow and Sorption Phenomena, *SPE Gas Technology Symposium*, Dallas, Texas, 7-9 June, *SPE Paper* 19102.
- Escobar F.H., Martinez J.A., Matilde M.M. (2013) Pressure Transient Analysis for a Reservoir with a Finite-conductivity Fault, *CT&F - Ciencia, Tecnologia y Futuro* 5, 2, 5-18.
- Everdingen V., Hust A.F. (1949) The Application of the Laplace Transformation to Flow Problems in Reservoirs, *Journal of Petroleum Technology* 1, 12, 305-324.
- Gringarten A.C., Ramey H., Raghavan R. (1974) Unsteady-state Pressure Distributions Created by a Well with a Single Infinite-conductivity Vertical Fracture, *SPE Journal* 14, 4, 347-360.
- Hu G.Z., Wang H.T., Fan X.G., Yuan Z.G., Hong S. (2009) Mathematical Model of Coalbed Gas Flow with Klinkenberg Effects in Multi-physical Fields and its Analytic Solution, *Transp. Porous Med.* 76, 3, 407-420.
- Kamal M.M., Six J.L. (1993) Pressure Transient Testing of Methane Producing Coalbeds (includes associated papers 28013 and 28155), *SPE Advanced Technology Series* 1, 1, 195-203.
- King G.R., Ertekin T., Schwerer F.C. (1986) Numerical Simulation of the Transient Behavior of Coal-seam Degasification Wells, *SPE Formation Evaluation* 1, 2, 165-183.
- Langmuir L. (1916) The Constitution of Fundamental Properties of Solids and Liquids, *J. Am. Chem. Soc.* 38, 11, 2221-2295.
- Meng L., Luke D.C. (2007) A Dual-porosity Model for Gas Reservoir Flow Incorporating Adsorption Behaviour - Part 1. Theoretical Development and Asymptotic Analyses, *Transp. Porous Med.* 68, 2, 153-173.
- Nie R.S., Meng Y.F., Guo J.C., Jia Y.L. (2012) Modeling Transient Flow Behavior of a Horizontal Well in a Coal seam, *International Journal of Coal Geology* 92, 1, 54-68.
- Ozkan E., Raghavan R. (1991a) New Solutions for Well-test-analysis Problems: Part 1-Analytical Considerations (includes associated papers 28666 and 29213), *SPE Formation Evaluation* 6, 3, 359-368.
- Ozkan E., Raghavan R. (1991b) New Solutions for Well-test-analysis Problems: Part 2- Computational Considerations and Applications, *SPE Formation Evaluation* 6, 3, 369-378.
- Rushing J.A., Blasingame T.A., Johnston J.L., Lee W.J. (1991) Slug Testing in Multiple Coal Seams Intersected by a Single, Vertical Fracture, *SPE Annual Technical Conference and Exhibition*, Dallas, Texas, 6-9 Oct., *SPE Paper* 22945-MS.
- Sarkar P.S., Rajtar J.M. (1994) Horizontal Well Transient Pressure Testing in Coalbed Reservoirs, *SPE Latin America/Caribbean Petroleum Engineering Conference*, Buenos Aires, Argentina, 27-29 April, *SPE Paper* 26995.
- Stehfest H. (1970) Numerical Inversion of Laplace Transforms, *Communications of the ACM* 13, 1, 47-49.
- US Energy Information Administration, Washington, DC; http://www.eia.gov/dnav/ng/hist/rngr52nus_1a.htm.
- Wang L., Wang X.D., Li J.Q., Wang J.H. (2013) Simulation of Pressure Transient Behavior for Asymmetrically Finite-conductivity Fractured Wells in Coal Reservoirs, *Transp. Porous Med.* 97, 3, 353-372.
- Zeng F.H., Zhao G. (2010) The Optimal Hydraulic Fracture Geometry Under Non-Darcy Flow Effects, *Journal of Petroleum Science and Engineering* 72, 1-2, 143-157.
- Zhang L.H., Zhao Y.L., Liu Q.G. (2014) Well-Test-Analysis and Applications of Source Functions in Bi-zonal Composite Gas Reservoir, *Petroleum Science and Technology* 32, 8, 965-973.
- Zhao Y.L., Zhang L.H., Wu F. (2012) Pressure Transient Analysis for Multi-Fractured Horizontal Well in Shale Gas Reservoirs, *Journal of Petroleum Science and Engineering* 90-91, 31-38.

Zhao Y.L., Zhang L.H., Luo J.X., Zhang B.N. (2014) Performance of fractured horizontal well with stimulated reservoir volume in unconventional gas reservoir, *Journal of Hydrology* **512**, 447-456.

Zhao Y.L., Zhang L.H., Zhao J.Z., Luo J.X., Zhang B.N. (2013a) “Triple porosity” Modeling of Transient Well Test and Rate Decline Analysis for Multi-fractured Horizontal Well in Shale Gas Reservoirs, *Journal of Petroleum Science and Engineering* **110**, 253-262.

Zhao Y.L., Zhang L.H., Wu F., Zhang B.N., Liu Q.G. (2013b) Analysis of Horizontal Well Pressure Behavior in Fractured Low Permeability Reservoirs with Consideration of Threshold Pressure Gradient, *Journal of Geophysics and Engineering* **10**, 3, 1-10.

Manuscript accepted in March 2014

Published online in September 2014

Cite this article as: Z. Yu-long, Z. Lie-Hui, F. Guo-Qing, Z. Bo-Ning and K. Bo (2014). Performance Analysis of Fractured Wells with Stimulated Reservoir Volume in Coal Seam Reservoirs, *Oil Gas Sci. Technol* **71**, 8.

APPENDIX

Derivation of Instantaneous Linear Source Function when a Well Produces at a Constant Production Rate

Substituting the dimensionless groups defined in Equations (12-32) into the governing Equations (2) and (4), the mathematical model to describe an instantaneous linear source with a constant rate is (Zhao *et al.*, 2014):

1 For Transient Diffusion

Inner region

$$\frac{1}{r_D} \frac{\partial}{\partial r_D} \left(r_D \frac{\partial \psi_{1f}}{\partial r_D} \right) = \frac{\omega_1}{M_{12}} \frac{\partial \psi_{1f}}{\partial t_D} + \frac{(1 - \omega_1 - \omega_2)(1 - \phi_{1f}) \alpha q_{sc} p_{sc} T}{M_{12} \lambda k_{f2} h T_{sc}} \frac{\partial V}{\partial r_{Dm}} \Big|_{r_{Dm}=1} \quad (\text{A1})$$

Outer region

$$\frac{1}{r_D} \frac{\partial}{\partial r_D} \left(r_D \frac{\partial \psi_{2f}}{\partial r_D} \right) = \omega_2 \frac{\partial \psi_{2f}}{\partial t_D} + \frac{(1 - \omega_1 - \omega_2)(1 - \phi_{2f}) \alpha q_{sc} p_{sc} T}{\lambda k_{f2} h T_{sc}} \frac{\partial V}{\partial r_{Dm}} \Big|_{r_{Dm}=1} \quad (\text{A2})$$

Using Fick's second law of diffusion, the partial differential equations describing transient state diffusive flow in the matrix are:

$$\frac{1}{r_{mD}^2} \frac{\partial}{\partial r_{mD}} \left(r_{mD}^2 \frac{\partial V_D}{\partial r_{mD}} \right) = \lambda \frac{\partial V_D}{\partial t_D} \quad (\text{A3})$$

The initial condition of the matrix system is:

$$V_D(t_D = 0) = 0 \quad (\text{A4})$$

The inner and outer boundary conditions of the coal particle are:

$$V_D(r_{mD} = 1) = V_D[\psi(p_f)] \quad (\text{A5})$$

$$\frac{\partial V_D}{\partial r_{mD}} \Big|_{r_{mD}=0} = 0 \quad (\text{A6})$$

Combining Equation (23) with Equations (A3-A6), we have:

$$\bar{V}_D(r_{mD}, t_D) = -\frac{\sigma \text{sh}(r_{mD} \sqrt{\lambda s})}{\text{sh}(\sqrt{\lambda s}) r_{mD}} \Delta \bar{\psi}(p_f) \quad (\text{A7})$$

So:

$$\frac{\partial \bar{V}_D}{\partial r_{Dm}} \Big|_{r_{Dm}=1} = -\sigma \left[\sqrt{\lambda s} \coth(\sqrt{\lambda s}) - 1 \right] \frac{k_{f2} h T_{sc} \Delta \bar{\psi}(p_f)}{\alpha q_{sc} p_{sc} T} \quad (\text{A8})$$

2 For Pseudo-Steady Flow

Inner region

$$\frac{1}{r_D} \frac{\partial}{\partial r_D} \left(r_D \frac{\partial \psi_{1f}}{\partial r_D} \right) = \frac{\omega_1}{M_{12}} \frac{\partial \psi_{1f}}{\partial t_D} + \frac{(1 - \omega_1 - \omega_2)(1 - \phi_{1f})}{M_{12}\lambda} \frac{\alpha q_{sc} p_{sc} T}{k_{f2} h T_{sc}} (V_E - V) \quad (\text{A9})$$

Outer region

$$\frac{1}{r_D} \frac{\partial}{\partial r_D} \left(r_D \frac{\partial \psi_{2f}}{\partial r_D} \right) = \omega_2 \frac{\partial \psi_{2f}}{\partial t_D} + \frac{(1 - \omega_1 - \omega_2)(1 - \phi_{2f})}{\lambda} \frac{\alpha q_{sc} p_{sc} T}{k_{f2} h T_{sc}} (V_E - V) \quad (\text{A10})$$

Using Fick's first law of diffusion, the partial differential equation describing pseudo-steady diffusive flow in the matrix is:

$$\lambda \frac{\partial V_D}{\partial t_D} = (V_{ED} - V_D) \quad (\text{A11})$$

Based in Equation (23) and using the Laplace transform method the solution of Equation (A-11) is:

$$\bar{V}_{ED} - \bar{V}_D = -\frac{\sigma s}{\lambda s + 1} \frac{k_{f2} h T_{sc} \Delta \bar{\psi}(p_f)}{\alpha q_{sc} p_{sc} T} \quad (\text{A12})$$

3 The Dimensionless Governing Equations

Inner region

$$\frac{1}{r_D} \frac{\partial}{\partial r_D} \left(r_D \frac{\partial \Delta \bar{\psi}_{1f}}{\partial r_D} \right) = f_1(s) \Delta \bar{\psi}_{1f} \quad (\text{A13})$$

The parameter groups of $f_1(s)$ for different diffusion models are:

$$f_1(s) = \frac{\omega_1 s}{M_{12}} + \frac{\beta_1 \sigma}{\lambda M_{12}} \left[\sqrt{\lambda s} \coth(\sqrt{\lambda s}) - 1 \right] \text{ for transient flow} \quad (\text{A14})$$

$$f_1(s) = \frac{\omega_1 s}{M_{12}} + \frac{\beta_1}{M_{12}} \frac{\sigma s}{\lambda s + 1} \text{ for pseudo-steady diffusion} \quad (\text{A15})$$

where $\beta_1 = (1 - \omega_1 - \omega_2)(1 - \phi_{1f})$

Outer region

$$\frac{1}{r_D} \frac{\partial}{\partial r_D} \left(r_D \frac{\partial \Delta \bar{\psi}_{2f}}{\partial r_D} \right) = \omega_2 s \Delta \bar{\psi}_{2f} + \frac{\beta_2}{\lambda} \sigma \left[\sqrt{\lambda s} \coth(\sqrt{\lambda s}) - 1 \right] \Delta \bar{\psi}_{2f} \quad (\text{A16})$$

The parameter groups of $f_2(s)$ for different diffusion models are:

$$f_2(s) = \omega_2 s + \frac{\beta_2 \sigma}{\lambda} \left[\sqrt{\lambda s} \coth \left(\sqrt{\lambda s} \right) - 1 \right] \quad \text{for transient flow} \quad (\text{A17})$$

$$f_2(s) = \omega_2 s + \beta_2 \frac{\sigma s}{\lambda s + 1} \quad \text{for pseudo-steady diffusion} \quad (\text{A18})$$

where $\beta_2 = (1 - \omega_1 - \omega_2)(1 - \phi_{2f})$

4 Solving the Mathematical Model

Inner region

$$\frac{1}{r_D} \frac{\partial}{\partial r_D} \left(r_D \frac{\partial \Delta \bar{\psi}_{1f}}{\partial r_D} \right) = f_1(s) \Delta \bar{\psi}_{1f} \quad (\text{A19})$$

Outer region

$$\frac{1}{r_D} \frac{\partial}{\partial r_D} \left(r_D \frac{\partial \Delta \bar{\psi}_{2f}}{\partial r_D} \right) = f_2(s) \Delta \bar{\psi}_{2f} \quad (\text{A20})$$

In the case of an infinitely large reservoir, the outer boundary condition is:

$$\Delta \bar{\psi}_{2f}(r_D, t_D)|_{r_D \rightarrow \infty} = 0 \quad (\text{A21})$$

According to characteristics of the Dirac delta function (Zhao *et al.*, 2012; Zhang *et al.*, 2014), the inner boundary condition becomes:

$$\lim_{\varepsilon \rightarrow 0^+} k_{1f} h \left(r_D \frac{\partial \bar{\psi}_{1f}}{\partial r_D} \right)_{r_D=\varepsilon} = -\alpha \hat{q} \frac{p_{sc} T}{T_{sc}} \frac{k_{2f}}{\Lambda L^2} \quad (\text{A22})$$

The interface the conditions defining pressure and flow rate continuity in the reservoir are expressed as follows:

$$\Delta \bar{\psi}_{1f}(r_D, t_D)|_{r_D=r_{mD}} = \Delta \bar{\psi}_{2f}(r_D, t_D)|_{r_D=r_{mD}} \quad (\text{A23})$$

and

$$\frac{\partial \Delta \bar{\psi}_{1f}}{\partial r_D} \Big|_{r_D=r_{mD}} = \frac{1}{M_{12}} \frac{\partial \Delta \bar{\psi}_{2f}}{\partial r_D} \Big|_{r_D=r_{mD}} \quad (\text{A24})$$

The general solution of Equation (A19) and Equation (A20) is:

$$\Delta \bar{\psi}_{1f} = A_1 I_0 \left(\sqrt{f_1(s)} r_D \right) + B_1 K_0 \left(\sqrt{f_1(s)} r_D \right) \quad (\text{A25})$$

$$\Delta \bar{\psi}_{2f} = A_2 I_0 \left(\sqrt{f_2(s)} r_D \right) + B_2 K_0 \left(\sqrt{f_2(s)} r_D \right) \quad (\text{A26})$$

According to the outer boundary condition (Eq. A21), we have:

$$A_2 = 0 \quad (\text{A27})$$

According to the inner boundary condition (Eq. A22), yields:

$$\lim_{\varepsilon \rightarrow 0^+} r_D \left[A_1 I_1 \left(\sqrt{sf_1(s)} r_D \right) - B_1 K_1 \left(\sqrt{sf_1(s)} r_D \right) \right]_{r_D=\varepsilon} = - \frac{\alpha}{k_{1f} h \sqrt{f_1(s)}} \hat{q} \frac{p_{sc} T}{T_{sc}} \frac{3.6 k_{2f}}{\Lambda L^2} \quad (\text{A28})$$

According to the characteristics of the Bessel function, $\lim_{x \rightarrow 0} x K_1(x) \rightarrow 1$, $\lim_{x \rightarrow 0} x I_1(x) \rightarrow 0$ gives:

$$B_1 = \alpha \hat{q} \frac{p_{sc} T}{T_{sc}} \frac{3.6 k_{2f}}{\Lambda L^2} \frac{1}{k_{1f} h} \quad (\text{A29})$$

Substituting Equations (A25) and (A26) into Equations (A23) and (A24):

$$A_1 I_0 \left(\sqrt{f_1(s)} r_{mD} \right) + B_1 K_0 \left(\sqrt{f_1(s)} r_{mD} \right) = B_2 K_0 \left(\sqrt{f_2(s)} r_{mD} \right) \quad (\text{A30})$$

$$A_1 I_1 \left(\sqrt{f_1(s)} r_{mD} \right) - B_1 K_1 \left(\sqrt{f_1(s)} r_{mD} \right) = -B_2 \frac{\sqrt{f_2(s)}}{M_{12} \sqrt{f_1(s)}} K_1 \left(\sqrt{f_2(s)} r_{mD} \right) \quad (\text{A31})$$

Combining Equations (A30) and (A31), yields:

$$A_1 = B_1 \frac{M_{12} \gamma_1 K_1(\gamma_1 r_{mD}) K_0(\gamma_2 r_{mD}) - \gamma_2 K_0(\gamma_1 r_{mD}) K_1(\gamma_2 r_{mD})}{M_{12} \gamma_1 I_1(\gamma_1 r_{mD}) K_0(\gamma_2 r_{mD}) + \gamma_2 I_0(\gamma_1 r_{mD}) K_1(\gamma_2 r_{mD})} \quad (\text{A32})$$

where: $\gamma_1 = \sqrt{f_1(s)}$, $\gamma_2 = \sqrt{f_2(s)}$

So:

$$\Delta \bar{\psi}_{1f} = \alpha \hat{q} \frac{p_{sc} T}{T_{sc}} \frac{3.6 k_{2f}}{\Lambda L^2} \frac{1}{\pi k_{1f} h} [K_0(\gamma_1 r_D) + A_C I_0(\gamma_1 r_D)] \quad (\text{A33})$$

where: $A_C = \frac{M_{12} \gamma_1 K_1(\gamma_1 r_{mD}) K_0(\gamma_2 r_{mD}) - \gamma_2 K_0(\gamma_1 r_{mD}) K_1(\gamma_2 r_{mD})}{M_{12} \gamma_1 I_1(\gamma_1 r_{mD}) K_0(\gamma_2 r_{mD}) + \gamma_2 I_0(\gamma_1 r_{mD}) K_1(\gamma_2 r_{mD})}$

If the outer boundary is closed, the solution can be easily obtained by replacing Equation (A21) with the following equation (Zhang *et al.*, 2014):

$$\left. \frac{\partial \Delta \bar{\psi}_{2f}}{\partial r_D} \right|_{r_D=r_{eD}} = 0 \quad (\text{A34})$$